MESHFREE ANALYSIS AND DIE SHAPE DESIGN OF EXTRUSION PROCESS

Nam H. Kim*, Ki-Young Yi§, and Kyung K. Choi¶
Department of Mechanical Engineering
University of Florida
PO Box 116300
Gainesville, FL 32611-6300

ABSTRACT

Meshfree analysis and die shape design of a 3-D metal extrusion problem is proposed. Multiplicatively decomposed elastoplasticity is used for the finite deformation nonlinear material model, while a penalty method is employed for the frictional contact condition between billet and die. The die shape design parameter in the CAD model is converted into a design velocity field on the rigid surface. The analytical design sensitivity formulation is derived in the continuum domain and is approximated using the meshfree method. A penalty-regularized contact variational equation is differentiated with respect to die shape design parameters. A material derivative consistent with the frictional return-mapping scheme is derived using non-associative plasticity. In order to improve the convergence behavior of the contact problem, a C^2-continous contact surface is constructed from the scattered set of particles, such that the contact and friction force change continuously.

KEYWORDS

Die Shape Design, Design Sensitivity Analysis, Frictional Contact, Smooth Surface Contact, Extrusion Process, Elastoplasticity

1. INTRODUCTION

Numerical simulation of a metal extrusion process using a Lagrangian formulation requires a finite-deformation elastoplastic constitutive relation and a flexible-rigid body contact condition on the interface.[1,2] Finite element-based numerical methods experience significant problems during large material deformation, in addition to a complicated elastoplastic evolution of the internal variables. In order to address these difficulties, a meshfree method is used to solve nonlinear equations during extrusion simulation.[3] In the meshfree method the structural domain is represented by a set of particles and the meshfree shape function is obtained from a set of supporting particles around an integration point to satisfy a reproducing condition, which exactly represents a certain order of polynomials. Since the construction of a shape function is independent of mesh geometry, the meshfree method is attractive for both large deformation and large shape-changing design problems, in which initially regular mesh may become significantly distorted during nonlinear analysis and the optimization process.[4]

A die shape sensitivity formulation of a 3-D contact problem is developed using a material derivative concept. If a structural component makes contact with other parts, the contact's effect on structural performance must be taken into account in the design. The die shape design parameter is first defined on the CAD model, and then converted into the design velocity field on the rigid surface. The die shape design parameter exerts its influence on structural performance through the contact constraint. For the purpose of structural analysis, the variational inequality is approximated using a penalty method, and the standard Newton-Raphason method is used to solve the nonlinear equation. The frictional mechanism is modeled using non-associative plasticity.[5] A material derivative of the variational equation is taken to obtain a design sensitivity equation that uses the same tangent operator as structural analysis at the converged configuration. By perturbing the rigid-body geometry, a die shape design sensitivity analysis can easily be performed.

A piecewise, linear contact surface creates significant difficulties in the Newton-type iterative method because it lacks continuity across the surface boundary. From a computational point of view, a C^1-continuous surface is required to guarantee a continuous contact force across the boundary. C^2-continuity is additionally required to provide a valid tangent stiffness matrix at each surface. In the finite element-based method, however, it is difficult to generate such regular surface patches. In this paper, a meshfree technique is used to produce a

* Assistant Professor, Member AIAA
§ Research Assistant, Center for Computer-Aided Design, University of Iowa, Iowa City, IA 52242
¶ Professor and Director, Associate Fellow AIAA, Center for Computer-Aided Design, University of Iowa, Iowa City, IA 52242

smooth surface from a set of scattered particles whose connectivity information is not provided in advance.[6]

The die shape design of a metal extrusion problem illustrates the efficiency and accuracy of the proposed sensitivity calculation method. The computational cost of sensitivity calculation is about 10~20% that of a response analysis. Accuracy of the proposed sensitivity computation is compared to that using the finite difference method.

2. CONTACT ANALYSIS

It has been shown that the contact variational inequality can be converted into the constrained optimization problem,[7] which in this paper is solved using the penalty regularization method.

2.1 Contact Kinematics

A brief review of contact analysis is presented to introduce notations that will appear in the subsequent DSA section. Throughout this paper, **X** represents the undeformed configuration, while **x** represents the current configuration. Figure 1 shows the contact situation between two bodies, represented by Ω_x^1 and Ω_x^2. Ω_x^1 is called a slave body, while Ω_x^2 is a master body, although such a distinction is inconsequential in continuum formulation. Likewise, part of the boundary Γ_x^1 in Ω_x^1 is called a slave surface, and part of the boundary Γ_x^2 in Ω_x^2 is called a master surface. The counterparts of Γ_x^1 and Γ_x^2 at the undeformed configuration will be denoted as Γ_X^1 and Γ_X^2, respectively. Contact constraints are imposed such that the points on Γ_x^1 cannot penetrate into Γ_x^2. Let the master surface Γ_x^2 be represented by the two parameters ξ_1 and ξ_2 such that a surface point $\mathbf{x}^c \in \Gamma_x^2$ can be expressed as $\mathbf{x}^c(\xi_1, \xi_2)$.

One of the most important steps in the contact analysis process is locating the contact point accurately and efficiently. The contact point $\mathbf{x}^c \in \Gamma_x^2$, corresponding to the slave point $\mathbf{x} \in \Gamma_x^1$, can be found from the following consistency condition:

$$\mathbf{e}_\alpha \cdot (\mathbf{x} - \mathbf{x}^c) = 0, \quad \alpha = 1, 2 \tag{1}$$

where $\mathbf{e}_\alpha$ is a tangential vector on the master surface, corresponding to parameter ξ_α (see Figure 1). Equation (1) provides the closest projection point $\mathbf{x}^c$ of **x**, and the corresponding parametric coordinates at the contact point are denoted by (ξ_1^c, ξ_2^c). For general surface Γ_x^2, no explicit form of the solution to (1) is available. Finding contact point $\mathbf{x}^c$ efficiently is very important for a large deformation problem. A local Newton method can be used to solve nonlinear equation (1) with a close initial estimate.

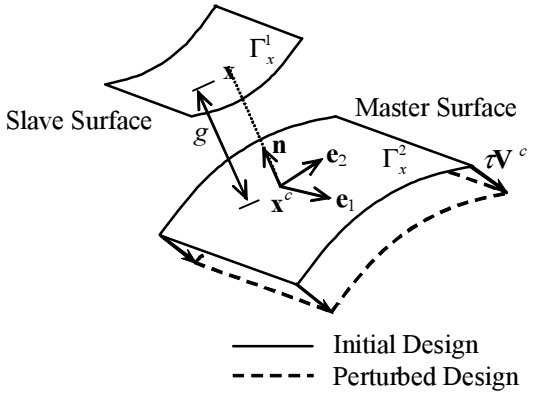

Figure 1 Contact kinematics and design perturbation

The gap function is defined as the distance between two contact points, namely,

$$g = \mathbf{n} \cdot (\mathbf{x} - \mathbf{x}^c) \geq 0 \tag{2}$$

where **n** is the unit normal vector at the contact point, and the inequality constraint represents the impenetrability condition, which states that the slave point cannot penetrate the slave surface. The violated region of constraint equation (2) will be penalized as shown in the following section.

2.2 Variational Formulation and Penalty Method

In the literature, the contact problem is described using the variational inequality. It is shown that the variational inequality is equivalent to the constrained minimization problem, which can be approximated using the Lagrange multiplier or penalty method.[7] In this paper, the penalty method is chosen to approximate the variational inequality, without introducing additional unknowns into the variational equation.

If a region $\Gamma_X^c (\subset \Gamma_X^1)$ exists that violates the impenetrability condition of (2), then it is penalized using the following penalty function:

$$P(\mathbf{x}, \mathbf{x}^c) = \frac{1}{2} \omega_N \int_{\Gamma_X^c} g^2 \, d\Gamma \tag{3}$$

where ω_N is the penalty parameter. Let the symbol "over-bar" denote a variation of the quantity such that $\bar{\mathbf{z}}$ represents the displacement variation. The variation of the penalty function in (3) contains the variation of the gap function, which can be obtained from its definition as

$$\bar{g} = \mathbf{n} \cdot \bar{\mathbf{z}} \tag{4}$$

Note that, due to the orthogonal condition, the variation of the normal vector vanishes. The variation of the penalty function in (3) leads to the contact form, defined as

$$\overline{P} \equiv b_N(\mathbf{z},\overline{\mathbf{z}}) = \omega_N \int_{\Gamma_x^c} g\mathbf{n}\cdot\overline{\mathbf{z}}\, d\Gamma \tag{5}$$

From a virtual work point of view, the contact form in (5) can be understood as the work done by contact force $\omega_N g\mathbf{n}$ during the virtual displacement $\overline{\mathbf{z}}$.

By using (5), the approximated variational equation for the penalized contact condition becomes

$$a_\Omega(\mathbf{z},\overline{\mathbf{z}}) + b_N(\mathbf{z},\overline{\mathbf{z}}) = \ell_\Omega(\overline{\mathbf{z}}), \qquad \forall\overline{\mathbf{z}} \in Z \tag{6}$$

Note that (6) is nonlinear even if a linear constitutive model is used, because the inequality constraint is imposed through the penalty method on the deformation field. In (6),

$$Z = \left\{ \mathbf{z} \in [H^1(\Omega)]^3 \,\middle|\, \mathbf{z}(\mathbf{x}) = \mathbf{0},\ \mathbf{x} \in \Gamma_g \right\} \tag{7}$$

is the space of kinematically admissible displacements, $H^1(\Omega)$ is first-order Sobolev space, and Γ_g is the essential boundary where the displacement is prescribed.

Since the purpose of this paper is to develop a contact design sensitivity analysis method, references will be provided for more detailed discussions of structural aspects. In this paper, an elastoplastic material with a combined isotropic and kinematic hardening model is used. In order to handle a finite deformation problem, it is assumed that the deformation gradient is constructed by multiplying elastic and plastic parts.[8]

2.3 Linearization

The nonlinear variational equation (6) can be solved using a Newton-Raphson iterative method through linearization. The exact tangent operator plays an important role in the convergence rate. Linearization of the structural energy form depends on the constitutive model, which can be found in the literature.[8] Let the linearization of a function $f(\mathbf{x})$ in the direction of $\Delta\mathbf{z}$ be denoted as

$$L[f] \equiv \frac{d}{d\varepsilon} f(\mathbf{x}+\varepsilon\Delta\mathbf{z})\bigg|_{\varepsilon=0} = \frac{\partial f}{\partial \mathbf{x}}\cdot\Delta\mathbf{z} \tag{8}$$

then, the linearization of $a_\Omega(\mathbf{z},\overline{\mathbf{z}})$ and $b_N(\mathbf{z},\overline{\mathbf{z}})$ becomes

$$L[a_\Omega(\mathbf{z},\overline{\mathbf{z}})] = a_\Omega^*(\mathbf{z};\Delta\mathbf{z},\overline{\mathbf{z}}) \tag{9}$$

$$L[b_N(\mathbf{z},\overline{\mathbf{z}})] = b_N^*(\mathbf{z};\Delta\mathbf{z},\overline{\mathbf{z}}) \tag{10}$$

where $\Delta\mathbf{z}$ is the displacement increment and $a_\Omega^*(\mathbf{z};\bullet,\bullet)$ is symmetric in its arguments. In the case of elastoplastic material, the expression of $a_\Omega^*(\mathbf{z};\Delta\mathbf{z},\overline{\mathbf{z}})$ is given in Simo[8]. The expression of $b_N^*(\mathbf{z};\Delta\mathbf{z},\overline{\mathbf{z}})$ can be found in Laursen and Simo.[9]

The linearization of the contact variational form in (10) is combined with that of the structural energy form in (9) to set up an incremental system of equations. Let the left superscript n denote the current configuration time t_n, and let the right superscript k denote the current iteration counter. The linearized incremental equation is

$$\begin{aligned} &a_\Omega^*({}^n\mathbf{z}^k;\Delta\mathbf{z}^{k+1},\overline{\mathbf{z}}) + b_N^*({}^n\mathbf{z}^k;\Delta\mathbf{z}^{k+1},\overline{\mathbf{z}}) \\ &\quad = \ell_\Omega(\overline{\mathbf{z}}) - a_\Omega({}^n\mathbf{z}^k,\overline{\mathbf{z}}) - b_N({}^n\mathbf{z}^k,\overline{\mathbf{z}}), \qquad \forall\overline{\mathbf{z}} \in Z \end{aligned} \tag{11}$$

For a given load step, (11) is solved iteratively until the right side (residual force) vanishes. After convergence, the decomposed tangent stiffness operator is stored to be used during DSA.

3. DESIGN SENSITIVITY ANALYSIS OF THE CONTACT PROBLEM

In this section, a die shape sensitivity formulation is developed for the contact variational equation using the material derivative approach. The basic formulas for material derivatives in nonlinear analysis can be found in Choi.[10] Even if a structure deforms during the nonlinear response analysis, the material derivative is always taken at the undeformed configuration. In the contact problem, transformation to the undeformed configuration is simple, using the relation $\mathbf{x} = \mathbf{X} + \mathbf{z}$ where $\mathbf{x}$ and $\mathbf{X}$ are spatial and material coordinates, respectively.

3.1 Material Derivative Formulas

In contrast to structural shape DSA, the geometry of the initial structure remains fixed during die shape DSA. Instead, the die geometry changes during design perturbation. Thus, a design velocity field $\mathbf{V}^c(\mathbf{X}^c)$ represents the design perturbation direction of the rigid body, and τ is a scalar parameter used to control perturbation size (see Figure 1). Since the contact constraint is related to the current coordinate of a material point, the following derivatives are required. The material derivative of structural point $\mathbf{x}\in\Omega_x$ at the current configuration becomes

$$\frac{d}{d\tau}(\mathbf{x}_\tau)\bigg|_{\tau=0} \equiv \frac{d}{d\tau}(\mathbf{X}+\mathbf{z}_\tau)\bigg|_{\tau=0} = \dot{\mathbf{z}}(\mathbf{X}) \tag{12}$$

The superposed dot (for example, $\dot{\mathbf{z}}$) will be used to denote the material derivative of a function. However, perturbation of the contact point $\mathbf{x}^c$ on the master surface Γ_x^c can be obtained using the chain rule and perturbing the natural coordinate corresponding to the contact point in the tangential direction, as

$$\frac{d}{d\tau}(\mathbf{x}_\tau^c)\bigg|_{\tau=0} = \mathbf{V}^c + \mathbf{e}_\alpha\dot{\xi}_\alpha \tag{13}$$

where a summation rule is used for the repeated indices. The contact point is perturbed while satisfying the contact consistency condition, in addition to its own design velocity fields.

The material derivatives of the structural energy and applied load form depend on which constitutive model is employed. For a general nonlinear material model that includes elastoplasticity, the material derivative of

the structural energy form can be expressed[11] as

$$\frac{d}{d\tau}\left[a_\Omega(\mathbf{z}_\tau,\bar{\mathbf{z}}_\tau)\right]\Big|_{\tau=0} = a^*_\Omega(\mathbf{z};\dot{\mathbf{z}},\bar{\mathbf{z}}) + a'_{\mathrm{V}}(\mathbf{z},\bar{\mathbf{z}}) \tag{14}$$

where, by replacing $\dot{\mathbf{z}}$ with $\Delta\mathbf{z}$, $a^*_\Omega(\mathbf{z};\dot{\mathbf{z}},\bar{\mathbf{z}})$ is the same form as the linearized structural energy form defined in (9). $a'_{\mathrm{V}}(\mathbf{z},\bar{\mathbf{z}})$ is the structural fictitious load form, which contains all known terms from response analysis and DSA up to the previous load step. Since the structural domain does not change, $a'_{\mathrm{V}}(\mathbf{z},\bar{\mathbf{z}})$ only has path-dependent terms. The material derivative of the applied load form is independent of displacement when a conservative load is considered:

$$\frac{d}{d\tau}\left[\ell_\Omega(\bar{\mathbf{z}}_\tau)\right]\Big|_{\tau=0} = 0 \tag{15}$$

Note that the structural fictitious load form $a'_{\mathrm{V}}(\mathbf{z},\bar{\mathbf{z}})$ is zero for elastic material. However, for elastoplastic material, $a'_{\mathrm{V}}(\mathbf{z},\bar{\mathbf{z}})$ requires the sensitivity results of the plastic variables at the previous load step, which makes DSA path-dependent.

3.2 Design Sensitivity Analysis of a Contact Problem

Instead of differentiating the variational inequality for contact DSA, the penalty-approximated variational equation is differentiated with respect to the die shape design parameter.

To begin, let the contact surface Γ^c_X change its shape due to design perturbation. The contact form in (5) depends on the design in two ways: explicitly through the contact surface change and implicitly through the state response $\mathbf{z}$. The material derivative of the contact form can be obtained as

$$\frac{d}{d\tau}\left[b_N(\mathbf{z}_\tau,\bar{\mathbf{z}}_\tau)\right]\Big|_{\tau=0} = \omega_n\int_{\Gamma^c_X}\left[\dot{g}\bar{g} + g\dot{\bar{g}} + g\bar{g}\kappa V^c_n\right]d\Gamma \tag{16}$$

where κ is the curvature of the master surface, and V^c_n is the normal component of the die shape design velocity. The purpose of the following derivations is to express $\dot{g}$ and $\dot{\bar{g}}$ in terms of $\dot{\mathbf{z}}$ and $\mathbf{V}^c$, and the implicit term $\dot{\mathbf{z}}$ can then be obtained in terms of the explicit term $\mathbf{V}^c$.

From its definition in (2), the material derivative of the gap function can be obtained as

$$\dot{g} = \mathbf{n}\cdot(\dot{\mathbf{z}} - \mathbf{V}^c) \tag{17}$$

Note that only $\dot{g}$ has a normal component of the variation. The material derivative of $\bar{g}$, however, is not straightforward. An outline of the derivation is provided as follows. From its definition in (4), it is necessary to differentiate the unit normal vector as

$$\frac{d}{d\tau}\mathbf{n}_\tau\Big|_{\tau=0} = -(\mathbf{n}\cdot\dot{\mathbf{e}}_\alpha)\mathbf{e}^\alpha \tag{18}$$

where $\mathbf{e}^\alpha$ is the dual basis of $\mathbf{e}_\alpha$. In (18),

$$\dot{\mathbf{e}}_\alpha \equiv \frac{d}{d\tau}(\mathbf{x}^c_{,\alpha})\Big|_{\tau=0} = \mathbf{V}^c_{,\alpha} + \mathbf{x}^c_{,\alpha\beta}\dot{\xi}_\beta \tag{19}$$

By using (18) and (19), the material derivative of $\bar{g}$ can be expressed as

$$\begin{aligned}\dot{\bar{g}} &= \frac{d}{d\tau}(\bar{\mathbf{z}}\cdot\mathbf{n})\Big|_{\tau=0} \\ &= -\mathbf{n}\cdot\dot{\mathbf{e}}_\alpha\bar{\xi}_\alpha + g(\mathbf{n}\cdot\dot{\mathbf{e}}_\beta)m^{-1}_{\alpha\beta}(\mathbf{n}\cdot\bar{\mathbf{e}}_\alpha)\end{aligned} \tag{20}$$

Thus, it is only necessary to calculate the expression of $\dot{\xi}_\alpha$ in terms of $\dot{\mathbf{z}}$ and $\mathbf{V}^c$. The expression of $\dot{\xi}_\alpha$ can be obtained by differentiating the consistency condition in (1) as

$$\frac{d}{d\tau}\left[(\mathbf{x}-\mathbf{x}^c)\cdot\mathbf{e}_\alpha\right]\Big|_{\tau=0} = 0, \quad \alpha = 1,2 \tag{21}$$

After rearrangement, $\dot{\xi}_\alpha$ is expressed in terms of $\dot{\mathbf{z}}$ and $\mathbf{V}^c$ as

$$\begin{aligned}\dot{\xi}_\alpha &= A^{-1}_{\alpha\beta}[\dot{\mathbf{z}}\cdot\mathbf{e}_\beta] + A^{-1}_{\alpha\beta}[-\mathbf{V}^c\cdot\mathbf{e}_\beta + g\mathbf{n}\cdot\mathbf{V}^c_{,\beta}] \\ &\equiv \xi_\alpha(\dot{\mathbf{z}}) + \xi_\alpha(-\mathbf{V}^c)\end{aligned} \tag{22}$$

with

$$A_{\alpha\beta} = m_{\alpha\beta} - g\mathbf{n}\cdot\mathbf{x}^c_{,\alpha\beta} \tag{23}$$

Note that $A_{\alpha\beta}$ is also the coefficient matrix that appears in the Newton iteration method in order to find the closest contact point in (1).

By substituting (22) into (20), and by using the expression of (17), the material derivative of the contact form can be expressed in terms of $\dot{\mathbf{z}}$ and $\mathbf{V}^c$. Since the objective of design sensitivity analysis is to solve the implicitly dependent parts in terms of the explicitly dependent ones, the material derivative of the contact form in (16) is separated into two parts, as

$$\frac{d}{d\tau}\left[b_N(\mathbf{z}_\tau,\bar{\mathbf{z}}_\tau)\right]\Big|_{\tau=0} \equiv b^*_N(\mathbf{z};\dot{\mathbf{z}},\bar{\mathbf{z}}) + b'_N(\mathbf{z},\bar{\mathbf{z}}) \tag{24}$$

where

$$\begin{aligned}b^*_N(\mathbf{z};\dot{\mathbf{z}},\bar{\mathbf{z}}) = {}& \omega_N\int_{\Gamma^c_X}\bar{\mathbf{z}}\cdot\mathbf{n}\mathbf{n}\cdot\dot{\mathbf{z}}\,d\Gamma \\ & -\omega_N\int_{\Gamma^c_X} g[\mathbf{n}\cdot\mathbf{x}^c_{,\alpha\beta}\bar{\xi}_\alpha\xi_\beta(\dot{\mathbf{z}})]\,d\Gamma \\ & +\omega_N\int_{\Gamma^c_X} g^2[(\mathbf{n}\cdot\mathbf{e}_\alpha(\dot{\mathbf{z}}))m^{-1}_{\alpha\beta}(\mathbf{n}\cdot\bar{\mathbf{e}}_\beta)]\,d\Gamma\end{aligned} \tag{25}$$

is the same as the linearized contact bilinear form used in (10) by replacing $\dot{\mathbf{z}}$ with $\Delta\mathbf{z}$, and the contact fictitious load $b'_N(\mathbf{z},\bar{\mathbf{z}})$ is defined as

$$b'_N(\mathbf{z},\bar{\mathbf{z}}) \equiv b^*_N(\mathbf{z};-\mathbf{V}^c,\bar{\mathbf{z}}) + \omega_N\int_{\Gamma^c_X}\kappa g\hat{\bar{\mathbf{z}}}\cdot\mathbf{n}V^c_n\,d\Gamma \tag{26}$$

Since form $b^*_N(\mathbf{z};\bullet,\bullet)$ is computed during response analysis, the same process can be used for design sensitivity analysis with different arguments.

The shape design sensitivity equation is obtained by taking the material derivative of (6) and by using the

relation in (14), (15), and (24) as

$$a_\Omega^*(\mathbf{z};\dot{\mathbf{z}},\overline{\mathbf{z}}) + b_N^*(\mathbf{z};\dot{\mathbf{z}},\overline{\mathbf{z}}) = -a_V'(\mathbf{z},\overline{\mathbf{z}}) - b_N'(\mathbf{z},\overline{\mathbf{z}}), \quad \forall \overline{\mathbf{z}} \in Z \tag{27}$$

Note that design sensitivity equation (27) is linear and symmetric with respect to its arguments, and is solved for each design parameter at a given load step. Each design parameter has a different design velocity field $\mathbf{V}^c$. The same system of equations is solved with different right sides. Since the left side of (27) is the same as that of (11) in response analysis, it is very efficient to solve a linear system of equations using an already factorized matrix.

4. FRICTIONAL CONTACT PROBLEM

When friction exists on the contact surface, the structure experiences a tangential traction force, in addition to the normal contact force in (5). Since frictional behavior is complicated, many idealizations have been made. The Coulomb friction law is one of the most frequently used methods to describe frictional behavior. However, it presents numerical difficulties due to frictional force discontinuity. A more advanced friction theory[9] assumes that frictional force elastically increases until reaching a limit value, at which point a macroscopic slip occurs along the contact surface. This theory corresponds to the non-associative flow rule in elastoplasticity. Thus, a similar return-mapping algorithm can be used to determine the frictional force. In this section, a design sensitivity formulation of this frictional model is developed.

4.1 Friction Model

Frictional force appears parallel to the contact surface and is expressed as

$$\mathbf{f} = f_\alpha \mathbf{e}^\alpha \tag{28}$$

The friction form of the contact problem can then be defined by multiplying the frictional force by the virtual relative slip[9] as

$$b_T(\mathbf{z},\overline{\mathbf{z}}) = \int_{\Gamma_x^c} f_\alpha \overline{\xi}_\alpha \, d\Gamma \tag{29}$$

The expression of $\overline{\xi}_\alpha$ can be obtained by taking the variation of consistency condition in (1) as

$$A_{\alpha\beta}\overline{\xi}_\alpha = \overline{\mathbf{z}} \cdot \mathbf{e}_\beta \tag{30}$$

From its definition in (23), the coefficient matrix $A_{\alpha\beta}$ contains the second-order derivative of the contact surface. Thus, the contact surface has to be C^2-continuous in order to have a continuous friction force. This regularity requirement of the contact surface will be discussed in detail in Section 5.

In the regularized friction model, frictional force f_α is calculated by using a return-mapping algorithm similar to that used for elastoplasticity. Initially, frictional force increases in proportion to the amount of relative slip. This trial frictional force is then compared with the limit value $\mu\omega_N g$. If the trial force is smaller than the limit value, then the trial force becomes the frictional force (stick condition). If the trial force is greater than the limit value, then the limit value is used as the frictional force (slip condition). Note that the direction of the frictional force is parallel to the trial force.

As with the frictionless contact problem, the nonlinear friction form in (29) has to be linearized as part of the implicit solution process. The linearized friction form is denoted by $b_T^*(\mathbf{z};\Delta\mathbf{z},\overline{\mathbf{z}})$, an expression that is developed in the subsequent section. If the following definitions are made

$$b_\Gamma(\mathbf{z},\overline{\mathbf{z}}) = b_N(\mathbf{z},\overline{\mathbf{z}}) + b_T(\mathbf{z},\overline{\mathbf{z}})$$
$$b_\Gamma^*(\mathbf{z};\Delta\mathbf{z},\overline{\mathbf{z}}) = b_N^*(\mathbf{z};\Delta\mathbf{z},\overline{\mathbf{z}}) + b_T^*(\mathbf{z};\Delta\mathbf{z},\overline{\mathbf{z}}) \tag{31}$$

then linearized incremental equation (11) can be extended to the frictional contact problem as

$$a_\Omega^*({}^n\mathbf{z}^k;\Delta\mathbf{z}^{k+1},\overline{\mathbf{z}}) + b_\Gamma^*({}^n\mathbf{z}^k;\Delta\mathbf{z}^{k+1},\overline{\mathbf{z}}) = \ell_\Omega(\overline{\mathbf{z}}) - a_\Omega({}^n\mathbf{z}^k,\overline{\mathbf{z}}) - b_\Gamma({}^n\mathbf{z}^k,\overline{\mathbf{z}}), \quad \forall \overline{\mathbf{z}} \in Z \tag{32}$$

It is shown in the next section that the same left side of (32) can be used in DSA.

4.2 Design Sensitivity Formulation of Frictional Form

Unlike the frictionless contact form in (5), the friction form depends on analysis results at the previous load step because of its updating algorithm. Thus, the sensitivity equation consists of three parts: implicitly dependent terms, explicitly dependent terms, and path-dependent terms. The material derivative of the friction form can be obtained from (29) as

$$\frac{d}{d\tau}[b_T(\mathbf{z},\overline{\mathbf{z}})]\bigg|_{\tau=0} = \int_{\Gamma_x^c} (\dot{f}_\alpha \overline{\xi}_\alpha + f_\alpha \dot{\overline{\xi}}_\alpha + \kappa f_\alpha \overline{\xi}_\alpha V_n^c)\, d\Gamma \tag{33}$$

As explained in Section 3.2, the last term in (33) can be calculated from analysis results and design velocity information. The expression of $\dot{\overline{\xi}}$ can be obtained by differentiating (30) with respect to the design parameter as

$$\begin{aligned} A_{\alpha\beta}\dot{\overline{\xi}}_\alpha = {} & -\mathbf{e}_\alpha \cdot \overline{\mathbf{z}}_{,\beta}\dot{\xi}_\beta - \mathbf{e}_\alpha \cdot (\dot{\mathbf{z}}_{,\beta} - \mathbf{V}_{,\beta}^c)\overline{\xi}_\beta \\ & -(\mathbf{e}_\alpha \cdot \mathbf{x}_{,\beta\gamma}^c - g\mathbf{n}\cdot\mathbf{x}_{,\alpha\beta\gamma}^c)\overline{\xi}_\beta\dot{\xi}_\gamma \\ & -\overline{\xi}_\beta \mathbf{e}_\beta \cdot \dot{\mathbf{e}}_\alpha - \dot{\xi}_\beta \mathbf{e}_\beta \cdot \overline{\mathbf{e}}_\alpha \\ & +g\mathbf{n}\cdot\overline{\mathbf{z}}_{,\alpha\beta}\dot{\xi}_\beta + g\mathbf{n}\cdot(\dot{\mathbf{z}}_{,\alpha\beta} - \mathbf{V}_{,\alpha\beta}^c)\overline{\xi}_\beta \\ & +\overline{\mathbf{z}}\cdot\dot{\mathbf{e}}_\alpha + (\dot{\mathbf{z}} - \mathbf{V}^c)\cdot\overline{\mathbf{e}}_\alpha \end{aligned} \tag{34}$$

Note that (34) includes the implicitly dependent term ($\dot{\mathbf{z}}$) and the explicitly dependent term ($\mathbf{V}^c$). No path-dependent term exists, and the expression is the same for both stick and slip conditions. Also note that the coefficient of the implicit and explicit term is the same,

which will be convenient in the sensitivity implementation stage.

With the stick condition, the traction force increases in proportion to the amount of relative slip between two contact surfaces. This increase corresponds to the elastic status of elastoplasticity. The material derivative of the frictional force contains three contributions:

$$\begin{aligned}\dot{f}_\alpha = {} & \omega_T \Phi_{\alpha\beta}\xi_\beta(\dot{\mathbf{z}}) && : \text{implicit} \\ & + \omega_T \Phi_{\alpha\beta}\xi_\beta(-\mathbf{V}^c) && : \text{explicit} \\ & + \dot{f}_\alpha^{n-1} + \omega_T M_{\alpha\beta}\xi_\beta^{n-1}(\dot{\mathbf{z}}) && : \text{path-dependent}\end{aligned} \tag{35}$$

where $\Phi_{\alpha\beta} = M_{\alpha\beta} + M_{\alpha\gamma,\beta}(\xi_\gamma - \xi_\gamma^{n-1})$. Thus, the material derivative of the frictional force depends on sensitivity results at the previous load step, which makes the sensitivity equation path-dependent. Again, note that the expressions of implicit and explicit terms are the same if $\dot{\mathbf{z}}$ is replaced by $\mathbf{V}^c$.

By substituting (34) and (35) into (33), the material derivative of the friction form is explicitly obtained in terms of $\dot{\mathbf{z}}$, $\mathbf{V}^c$, and the path-dependent terms, as

$$\left.\frac{d}{d\tau}[b_T(\mathbf{z},\overline{\mathbf{z}})]\right|_{\tau=0} \equiv b_T^*(\mathbf{z};\dot{\mathbf{z}},\overline{\mathbf{z}}) + b_T'(\mathbf{z},\overline{\mathbf{z}}) \tag{36}$$

where the linearized friction form is defined by collecting all terms that include $\dot{\mathbf{z}}$ as

$$\begin{aligned} b_T^*(\mathbf{z};\dot{\mathbf{z}},\overline{\mathbf{z}}) = \int_{\Gamma_X^c} \{ & \omega_T \Phi_{\alpha\beta}\overline{\xi}_\alpha \xi_\beta(\dot{\mathbf{z}}) + f_\gamma A_{\alpha\gamma}^{-1}[-\mathbf{e}_\alpha \cdot \overline{\mathbf{z}}_{,\beta}\xi_\beta(\dot{\mathbf{z}}) \\ & - \mathbf{e}_\alpha \cdot \dot{\mathbf{z}}_{,\beta}\overline{\xi}_\beta - (\mathbf{e}_\alpha \cdot \mathbf{x}_{,\beta\zeta}^c - g\mathbf{n}\cdot\mathbf{x}_{,\alpha\beta\zeta}^c)\overline{\xi}_\beta\xi_\zeta(\dot{\mathbf{z}}) \\ & - \overline{\xi}_\beta \mathbf{e}_\beta \cdot \mathbf{e}_\alpha(\dot{\mathbf{z}}) - \xi_\beta(\dot{\mathbf{z}})\mathbf{e}_\beta \cdot \overline{\mathbf{e}}_\alpha + g\mathbf{n}\cdot\overline{\mathbf{z}}_{,\alpha\beta}\xi_\beta(\dot{\mathbf{z}}) \\ & + g\mathbf{n}\cdot\dot{\mathbf{z}}_{,\alpha\beta}\overline{\xi}_\beta + m_{\beta\zeta}^{-1}(\overline{\mathbf{z}}\cdot\mathbf{e}_\beta\mathbf{e}_\zeta\cdot\dot{\mathbf{z}}_{,\alpha} + \dot{\mathbf{z}}\cdot\mathbf{e}_\beta\mathbf{e}_\zeta\cdot\overline{\mathbf{z}}_{,\alpha}) \\ & + \overline{\mathbf{z}}\cdot\mathbf{nn}\cdot\mathbf{e}_\alpha(\dot{\mathbf{z}}) + \overline{\mathbf{e}}_\alpha\cdot\mathbf{nn}\cdot\dot{\mathbf{z}}]\}\, d\Gamma \end{aligned} \tag{37}$$

and the friction fictitious load is obtained by collecting those explicitly dependent terms and path-dependent terms as

$$\begin{aligned} b_T'(\mathbf{z},\overline{\mathbf{z}}) = {} & b_T^*(\mathbf{z};-\mathbf{V}^c,\overline{\mathbf{z}}) + \int_{\Gamma_X^c} \kappa f_\alpha \overline{\xi}_\alpha V_n^c \, d\Gamma \\ & + \int_{\Gamma_X^c} (\dot{f}_\alpha^{n-1}\overline{\xi}_\alpha + \omega_T M_{\alpha\beta}\overline{\xi}_\alpha\dot{\xi}_\beta^{n-1})\, d\Gamma \end{aligned} \tag{38}$$

Note that the last integral represents those path-dependent terms that are obtained from the design sensitivity results at the previous load step t_{n-1}.

With the slip condition, the magnitude of the frictional force is determined from the normal contact force, while the applied direction still runs parallel to the trial force. From the return-mapping algorithm, the material derivative of the frictional force for the slip condition can be obtained as

$$\begin{aligned} \dot{f}_\alpha = {} & \mu\omega_N p_\alpha \mathbf{n}\cdot(\dot{\mathbf{z}} - \mathbf{V}^c) \\ & + \frac{\mu\omega_N g}{\|\mathbf{f}^{tr}\|}[\dot{f}_\alpha^{tr} - p_\alpha p^\beta \dot{f}_\beta^{tr} - f_\alpha^{tr} p_\alpha \mathbf{p}\cdot\dot{\mathbf{e}}^\beta] \end{aligned} \tag{39}$$

where $\dot{f}_\alpha^{tr}$ is exactly the same as in (35) for the stick condition. By substituting Eqs. (34) and (39) into Eq. (33), the material derivative of the friction form is obtained. If the implicitly dependent terms are combined, then the following linearized friction form is defined:

$$\begin{aligned} & b_T^*(\mathbf{z};\dot{\mathbf{z}},\overline{\mathbf{z}}) = \\ & \mu\omega_N \int_{\Gamma_X^c} [\mathbf{n}\cdot\dot{\mathbf{z}} p_\alpha \overline{\xi}_\alpha - \omega_T g(\delta_\alpha^\beta - p_\alpha p^\beta)\Phi_{\beta\gamma}\overline{\xi}_\alpha\xi_\gamma(\dot{\mathbf{z}})/\|\mathbf{f}^{tr}\|]\, d\Gamma \\ & + \mu\omega_N \int_{\Gamma_X^c} g p_\alpha p^\beta \overline{\xi}_\alpha(\dot{\mathbf{z}}_{,\alpha}\cdot\mathbf{p} - \mathbf{x}_{,\alpha\beta}^c\cdot\mathbf{p}\xi_\beta(\dot{\mathbf{z}}))\, d\Gamma \\ & + \int_{\Gamma_X^c} f_\gamma A_{\alpha\gamma}^{-1}[-\mathbf{e}_\alpha\cdot\overline{\mathbf{z}}_{,\beta}\xi_\beta(\dot{\mathbf{z}}) - \mathbf{e}_\alpha\cdot\dot{\mathbf{z}}_{,\beta}\overline{\xi}_\beta \\ & \quad - (\mathbf{e}_\alpha\cdot\mathbf{x}_{,\beta\zeta}^c - g\mathbf{n}\cdot\mathbf{x}_{,\alpha\beta\zeta}^c)\overline{\xi}_\beta\xi_\zeta(\dot{\mathbf{z}}) - \overline{\xi}_\beta\mathbf{e}_\beta\cdot\mathbf{e}_\alpha(\dot{\mathbf{z}}) \\ & \quad - \xi_\beta(\dot{\mathbf{z}})\mathbf{e}_\beta\cdot\overline{\mathbf{e}}_\alpha + g\mathbf{n}\cdot\overline{\mathbf{z}}_{,\alpha\beta}\xi_\beta(\dot{\mathbf{z}}) + g\mathbf{n}\cdot\dot{\mathbf{z}}_{,\alpha\beta}\overline{\xi}_\beta \\ & \quad + m_{\beta\zeta}^{-1}(\overline{\mathbf{z}}\cdot\mathbf{e}_\beta\mathbf{e}_\zeta\cdot\dot{\mathbf{z}}_{,\alpha} + \dot{\mathbf{z}}\cdot\mathbf{e}_\beta\mathbf{e}_\zeta\cdot\overline{\mathbf{z}}_{,\alpha}) \\ & \quad + \overline{\mathbf{z}}\cdot\mathbf{nn}\cdot\mathbf{e}_\alpha(\dot{\mathbf{z}}) + \overline{\mathbf{e}}_\alpha\cdot\mathbf{nn}\cdot\dot{\mathbf{z}}]\, d\Gamma \end{aligned} \tag{40}$$

In a similar way, the explicitly dependent terms and path-dependent terms are combined to define the friction fictitious load as

$$\begin{aligned} b_T'(\mathbf{z},\overline{\mathbf{z}}) = {} & b_T^*(\mathbf{z};-\mathbf{V}^c,\overline{\mathbf{z}}) + \int_{\Gamma_X^c} \kappa f_\alpha \overline{\xi}_\alpha V_n^c \, d\Gamma \\ & + \mu\omega_N \int_{\Gamma_X^c} \frac{g\overline{\xi}_\beta}{\|\mathbf{f}^{tr}\|}(\delta_\alpha^\beta - p_\alpha p^\beta)(\dot{f}_\alpha^{n-1} + \omega_T M_{\alpha\gamma}\dot{\xi}_\gamma^{n-1})\, d\Gamma \end{aligned} \tag{41}$$

The last integral in (41) represents path-dependent terms. It is interesting to note that the form $b_T^*(\mathbf{z};\dot{\mathbf{z}},\overline{\mathbf{z}})$ from the stick condition in (37) is symmetric with respect to its arguments, while $b_T^*(\mathbf{z};\dot{\mathbf{z}},\overline{\mathbf{z}})$ from the slip condition in (40) is not symmetric. This is due to the non-associative plastic return-mapping algorithm.

By adding (26) and (38) for the stick condition, or (26) and (41) for the slip condition, the following form can be defined:

$$b_V'(\mathbf{z},\overline{\mathbf{z}}) = b_N'(\mathbf{z},\overline{\mathbf{z}}) + b_T'(\mathbf{z},\overline{\mathbf{z}}) \tag{42}$$

Equation (42) represents the explicitly dependent and path-dependent terms of the contact condition. As mentioned before, since the explicitly dependent terms have the same form as the implicitly dependent ones, $b_V'(\mathbf{z},\overline{\mathbf{z}})$ uses the same contact stiffness matrix from the contact analysis. Only path-dependent terms need to be calculated separately.

By adding the material derivative of the friction form in (36) to (27), the design sensitivity equation for the frictional contact problem is obtained as

$$\begin{aligned} & a_\Omega^*(\mathbf{z};\dot{\mathbf{z}},\overline{\mathbf{z}}) + b_\Gamma^*(\mathbf{z};\dot{\mathbf{z}},\overline{\mathbf{z}}) \\ & \qquad = -a_V'(\mathbf{z},\overline{\mathbf{z}}) - b_V'(\mathbf{z},\overline{\mathbf{z}}), \quad \forall\overline{\mathbf{z}} \in Z \end{aligned} \tag{43}$$

This design sensitivity equation solves the material derivative $\dot{\mathbf{z}}$ for each design variable. Since the left side of (43) is same as the left side of (32), the design sensitivity equation uses the same stiffness matrix as the response analysis that already has a factorized form. After

solving for $\dot{\mathbf{z}}$ at load step t_n, the path dependent terms have to be updated for the next time step. Since path-dependency comes from the frictional force update, the material derivative $\dot{f}_\alpha$ in (35) or in (39) has to be stored. It is not necessary to store the material derivative $\dot{\xi}_\alpha$, since (22) can be used from the calculated $\dot{\mathbf{z}}$. In addition to the frictional effect, the plastic variables of elastoplasticity are path-dependent, and their material derivatives have to be updated accordingly.[11]

5. SMOOTH CONTACT SURFACE

In the development of a continuum-based contact analysis and design sensitivity formulation, it can easily be seen that the expression of the contact force in (29) contains the second-order derivative of the master surface, while the linearized contact form in (37) and (40) contains the third-order derivative. Thus, in order to have a continuous contact force as well as a stable Newton method, the master surface should have at least C^2-continuity. If a conventional finite element-based contact surface representation method is used, discontinuity may occur because it is difficult to impose a C^2-countinuity across the element boundary. One remedy for this difficulty is to generate a C^2-continous spline surface using finite element nodes as control points.[12] However, this approach requires that an $n\times m$ regular array of nodes and meshes be applied to the three-dimensional contact surface. Wang[6] proposed a method to generate a smooth surface from a scattered set of particles without requiring mesh connectivity.

In this paper, a smooth master surface is generated by using a meshfree interpolation function. Since design sensitivity equation (43) is developed based on the continuum geometry, the same formulation can apply to either a piecewise linear surface or a smooth surface without modification. The sensitivity formulation only requires information that is already available from contact analysis. However, if a discrete design sensitivity formulation is used, then differentiation of the surface generation process has to be taken into account, which is not only complicated but strongly depends on the analysis code.

Figure 2 illustrates the process for constructing a smooth surface from a set of scattered particles using a meshfree shape function $\Psi(\xi_1,\xi_2)$. At a given slave particle $\mathbf{x}$, an NP number of master particles close to the slave particle is selected to construct a local surface. These master particles are then projected onto a parametric plane using the least-square method. In the parametric plane, a meshfree interpolation is carried out using those projected particles. Let (ξ_1^I,ξ_2^I), I=1,…,NP be the parametric coordinates of the projected particles. The meshfree shape function can be obtained by imposing the reproducing condition as

$$\Psi_I(\xi_1,\xi_2)=\mathbf{H}^T(0,0)\mathbf{M}^{-1}(\xi_1,\xi_2) \times\mathbf{H}(\xi_1-\xi_1^I,\xi_2-\xi_2^I)\Phi_a(\xi_1-\xi_1^I,\xi_2-\xi_2^I) \tag{44}$$

where $\mathbf{H}(\xi_1,\xi_2)$ is the monomial basis vector and is determined according to the order of the consistency condition. In the case in which the second-order consistency condition is used, the basis vector becomes

$$\mathbf{H}(\xi_1,\xi_2)=[1 \quad \xi_1 \quad \xi_2 \quad \xi_1^2 \quad \xi_1\xi_2 \quad \xi_2^2]^T \tag{45}$$

The moment matrix $\mathbf{M}(\xi_1,\xi_2)$ in (44) is defined as

$$\mathbf{M}(\xi_1,\xi_2)=\sum_{I=1}^{NP}\mathbf{H}(\xi_1-\xi_1^I,\xi_2-\xi_2^I) \times\mathbf{H}^T(\xi_1-\xi_1^I,\xi_2-\xi_2^I)\Phi_a(\xi_1-\xi_1^I,\xi_2-\xi_2^I) \tag{46}$$

Since matrix inversion is involved in (44), it is important to note that NP has to be large enough so that the matrix $\mathbf{M}^{-1}$ is not singular. Finally, the kernel function $\Phi_a(\xi_1,\xi_2)$ determines the smoothness of the shape function $\Psi(\xi_1,\xi_2)$. Since a minimum of C^2-continuity is required for the master surface, the kernel function can be selected from the C^2 cubic B-spline function or from the C^∞ Gaussian function.

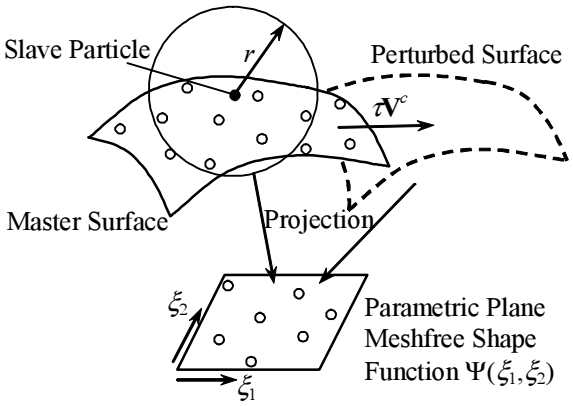

Figure 2 Smooth contact surface from a scatter set of particles

After generating the meshfree shape function in the parametric domain, physical coordinates and the tangential vectors of the master surface can be interpolated using

$$\mathbf{x}(\xi_1,\xi_2)=\sum_{I=1}^{NP}\Psi_I(\xi_1,\xi_2)\mathbf{x}_I \tag{47}$$

$$\mathbf{x}_{,\alpha}(\xi_1,\xi_2)=\sum_{I=1}^{NP}\frac{d\Psi_I(\xi_1,\xi_2)}{d\xi_\alpha}\mathbf{x}_I \tag{48}$$

Thus, all geometric variables that appear in previous sections can be calculated.

6. EXTRUSION DIE SHAPE DESIGN

A design problem of the extrusion problem is considered in order to improve product quality and to reduce processing costs. Product quality is related to the final

product shape and the regularity of the product's mechanical properties. The processing cost is related to the process control force, deformation work, or deformation efficiency. In addition, process limits have to be considered in the design stage, such as the maximum contact stress level that will result in die failure and punch buckling.

In this example, a forward solid extrusion problem, as illustrated in Figure 3, is considered. In displacement-driven nonlinear analysis, the vertical displacement of the billet's upper surface is controlled to push it down. The reaction force on the billet's top surface is then measured as the process control force. Because of symmetry, a quarter model is used with symmetric boundary conditions. The ratio of the area reduction is 2.65, and the initial die angle is 30°. The whole die surface is modeled with 612 particles, and a smooth contact surface is locally generated based on the meshfree approximation method in (47). A contact constraint is imposed between the billet's outer surface and the extrusion die surface with a frictional coefficient of μ = 0.05.

Figure 4 shows the deformation history and effective plastic strain at the final configuration. The maximum effective plastic strain appears at the outer surface of the billet with a magnitude of 2.68. The initial billet length of 0.6 m is extended to 1.6583 m at the final configuration, which represents a 276% extension. This extension ratio conforms to the area reduction ratio of 2.65 and to the maximum plastic strain of 2.68.

Since the extrusion process generates the desired final shape from a circular billet, design parameters are largely limited to the extrusion die shape and material property. The latter can be considered since it is possible to adjust the material property by changing the process temperature. In addition, the frictional coefficient can be considered a design parameter. In this example, die shape represents die depth, die angle, and dead zone fillet radius. As illustrated in Figure 5, three design parameters are defined on the circular die. As explained in Section 3, the design velocity field that corresponds to the design parameter must be defined on the extrusion die surface. Figure 5 shows the vector plots of three design parameters. As the design changes, particle points on the die surface will move in the direction of the design velocity vector.

Design sensitivity analysis is carried out using the design velocity fields defined in Figure 5. The process work and maximum plastic strain are chosen as performance measures. The computational cost of design sensitivity analysis is about 10% of the response analysis cost per design parameter. Table 2 shows the design sensitivity of the process force and the maximum effective plastic strain. The design parameter u_1 contributes most significantly to the process force, while the design parameters u_2 and u_3 contribute most to the effective plastic strain.

Since the design parameter u_1 (the die angle) contributes most to the process work, a new updated design is generated by reducing the die angle to 27°, which is a 10% reduction from the initial design. Figure 6 shows normalized extrusion process forces at initial and new designs. The area covered by the process force is the process work. As expected from design sensitivity results, the process work is reduced by 4.5% for the new design.

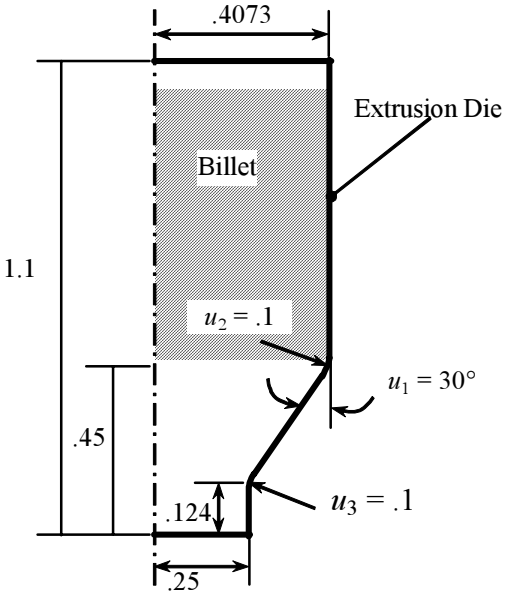

Figure 3 Design parameterization of circular-circular extrusion

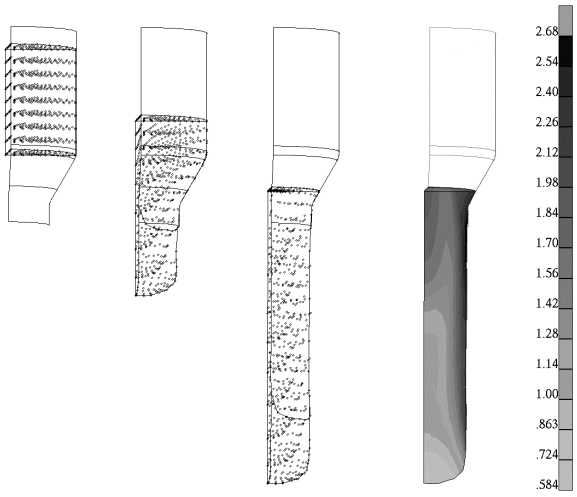

Figure 4 Deformation history and effective plastic strain of the extrusion problem

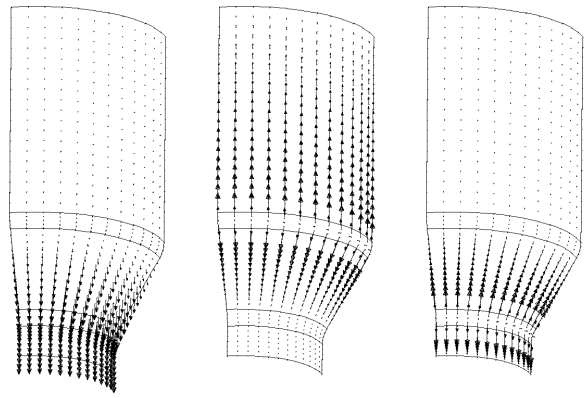

(a) u_1 (b) u_2 (c) u_3

Figure 5 Die shape design velocity fields

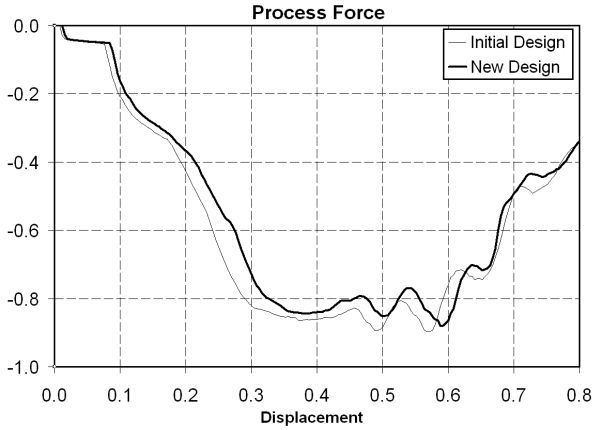

Figure 6 Extrusion process forces at the initial and new designs

Table 2 Relative design sensitivity results for the extrusion problem

Design Parameter	Process Work Sensitivity	Plastic Strain Sensitivity
u_1	−5.50E−3	−5.32E−2
u_2	6.60E−4	−6.24E−3
u_3	−6.65E−5	−1.10E−4

7. CONCLUSION

A meshfree analysis and die shape design procedure for the metal extrusion problem has been developed. Since the explicitly dependent terms have the same expression as appears in the linearization process, matrix information from contact analysis is readily used for design sensitivity purposes. However, the path-dependent terms must be derived separately when friction exists between contact interfaces. Since the continuum-based formulation is used, differentiation of the complicated smooth surface construction process was unnecessary, and virtually any surface construction method is applicable without modifying the formulation. The accuracy and efficiency of sensitivity information is compared with finite difference results with excellent agreement.

ACKNOWLEDGEMENT

This research is supported by NSF/DARPA Optimized Portable Algorithms and Applications Libraries (OPAAL) with contract No. 9874015.

REFERENCE

1. N. H. Kim, K. K. Choi, and J. S. Chen, Structural Optimization of Finite Deformation Elastoplasticity: Continuum-Based Design Sensitivity Formulation, Computers and Structures, Vol. 79, No. 20-21, pp. 1959–1976, 2001
2. K. K. Choi and N. H. Kim, Design Optimization of Springback in a Deepdrawing Process, AIAA Journal, Vol. 40, No. 1, pp. 147-153, 2002
3. J. S. Chen, C. Pan, C. M. D. L. Roque, and H. –P. Wang, A Lagrangian Reproducing Kernel Particle Method for Metal Forming Analysis, Computational Mechanics. Vol. 22, 289-307, 1998
4. N. H. Kim, K. K. Choi, and M. Botkin, Numerical Method for Shape Optimization Using Meshfree Method, Structural and Multidisciplinary Optimization, accepted, 2002
5. R. Michalowski and Z. Mroz, Associated and Non-associated Sliding Rules in Contact Friction Problems, Archives of Mechanics, Vol. 30, 259–276, 1978
6. H. P. Wang, Meshfree Smooth Contact Formulation and Boundary Condition Treatments in Multi-Body Contact, Ph.D. Thesis, The University of Iowa, Iowa City, IA, 2000
7. N. Kikuchi and J. T. Oden, Contact Problems in Elasticity: A Study of Variational Inequalities and Finite Element Method, SIAM, Philadelphia, PA, 1988
8. J. C. Simo, Algorithms for Static and Dynamic Multiplicative Plasticity That Preserve the Classical Return Mapping Schemes of the Infinitesimal Theory, Computer Methods in Applied Mechanics and Engineering **99**, 61–112, 1992
9. Laursen, T.A. and Simo, J.C., 1993, A Continuum-based Finite Element Formulation for the Implicit Solution of Multibody, Large Deformation Frictional Contact Problems, International Journal for Numerical Methods in Engineering **36**, 2451–3485

10. Choi K.K., 1993, Design Sensitivity Analysis of Nonlinear Structures II, Structural Optimization: Status & Premises, AIAA Progress in Astronautics and Aeronautics **150**, Chapter 16, 407–446

11. Kim, N.H., Choi, K.K., Chen, J.S., 2001, Structural Optimization of Finite Deformation Elastoplasticity Using Continuum-Based Shape Design Sensitivity Formulation, Computers & Structures, Vol. 39, No. 8, pp. 2087-2108, 2002

12. Hanssen, E. and Klarbring, A., 1990, Rigid Contact Modeled by CAD Surface, Eng. Computations **7**, 344–348

Table 1 Accuracy of design sensitivity results

Design	Performance	ψ	$\Delta\psi$	$\psi/\Delta\tau$	$\Delta\psi/\psi/\Delta\tau\times100$
u_1	z_{344}	-7.66403	-8.74269E-7	-8.74284E-7	100.00
	z_{331}	-7.11372	-8.70281E-7	-8.70297E-7	100.00
	z_{319}	-6.46946	-8.41994E-7	-8.42008E-7	100.00
	z_{307}	-5.78084	-7.79330E-7	-7.79347E-7	100.00
	z_{295}	-5.07427	-6.83249E-7	-6.83270E-7	100.00
	z_{283}	-4.36168	-5.64229E-7	-5.64249E-7	100.00
	z_{271}	-3.64779	-4.38470E-7	-4.38491E-7	100.00
	z_{259}	-2.93541	-3.23620E-7	-3.23641E-7	99.99
	z_{286}	-4.33574	-5.13241E-7	-5.13267E-7	100.00
	z_{312}	-5.77780	-7.17279E-7	-7.17305E-7	100.00
u_2	z_{344}	-7.66403	1.01763E-6	1.01722E-6	100.04
	z_{331}	-7.11372	9.93909E-7	9.93374E-7	100.05
	z_{319}	-6.46946	9.34760E-7	9.34128E-7	100.07
	z_{307}	-5.78084	8.48858E-7	8.48161E-7	100.08
	z_{295}	-5.07427	7.46921E-7	7.46197E-7	100.10
	z_{283}	-4.36168	6.36105E-7	6.35389E-7	100.11
	z_{271}	-3.64779	5.21189E-7	5.20510E-7	100.13
	z_{259}	-2.93541	4.05932E-7	4.05317E-7	100.15
	z_{286}	-4.33574	6.24759E-7	6.23955E-7	100.13
	z_{312}	-5.77780	8.39500E-7	8.38630E-7	100.10
u_3	z_{344}	-7.66403	-1.73855E-7	-1.73653E-7	100.12
	z_{331}	-7.11372	-3.13213E-7	-3.12915E-7	100.10
	z_{319}	-6.46946	-5.02555E-7	-5.02153E-7	100.08
	z_{307}	-5.78084	-7.15329E-7	-7.14828E-7	100.07
	z_{295}	-5.07427	-9.30001E-7	-9.29415E-7	100.06
	z_{283}	-4.36168	-1.13062E-6	-1.12997E-6	100.06
	z_{271}	-3.64779	-1.30268E-6	-1.30198E-6	100.05
	z_{259}	-2.93541	-1.43077E-6	-1.43006E-6	100.05
	z_{286}	-4.33574	-1.46946E-6	-1.46873E-6	100.05
	z_{312}	-5.77780	-1.28150E-6	-1.28086E-6	100.05